Patient-derived mesenchymal stromal cells establish an IL-6 axis that marks progression from smouldering to active multiple myeloma

Patient-derived mesenchymal stromal cells establish an IL-6 axis that marks progression from smouldering to active multiple myeloma

Phoebe Elizabeth Blair[1], Tianyuan Chu[1], Andrew Robinson[2], Khalid Saja[2], Stuart Rushworth[3], Ralf Michael Zwacka[1,#,*], Andrea Mohr[1,#,*]

[1]School of Life Sciences, Protein Structure and Mechanisms of Disease Group, Cancer and Stem Cell Biology Group, University of Essex, Colchester, CO4 3SQ, UK

[2]Haematology Department, East Suffolk and North Essex NHS Foundation Trust, Colchester CO4 5JL, UK.

[3]Metabolic Health Research Centre, Norwich Medical School, University of East Anglia, Norwich NR4 7UQ, UK

# equally contributed

Corresponding author:

*CONTACT: rzwacka@essex.ac.uk/amohr@essex.ac.uk
Ralf Michael Zwacka/Andrea Mohr
University of Essex
School of Life Sciences
Cancer and Stem Cell Biology Group
Colchester
Essex CO4 3SQ
United Kingdom

Abstract

IL-6 signalling in the bone marrow (BM) is compartmentalised. Different cell populations within the BM niche contribute distinct components of the IL-6 signalling network, yet how their roles change during myeloma progression has remained unclear. We examined how the respective contributions of mesenchymal stromal cells (MSCs) and primary multiple myeloma (MM) cells to the IL-6 signalling machinery change during disease progression. MSCs were identified as the principal source of IL-6, whereas MM cells secreted minimal IL-6 but were the primary source of soluble IL-6 receptor (sIL-6R). This functional interplay, with MSCs supplying the ligand and MM cells providing the soluble receptor, establishes a paracrine IL-6 trans-signalling axis. The contribution of MM cells to this axis increases significantly with disease stage: cells from patients with active MM secreted substantially greater quantities of sIL-6R than those from patients with smouldering disease, identifying sIL-6R as a marker of biologically active disease. This increase is mirrored by higher basal IL-6 secretion from MSCs in advanced disease, demonstrating augmentation of the IL-6 signalling pathway as disease progresses. Using Hyper-IL-6 and sgp130, we demonstrated that trans-signalling through gp130 is the dominant mechanism by which stromal-derived IL-6 protects MM cells from treatment-induced apoptosis, independent of membrane-bound IL-6R expression. Therefore, targeted inhibition of IL-6 trans-signalling with sgp130 could be used to suppress pathogenic effects in MM while preserving beneficial classical IL-6 signalling, offering a more precise and potentially safer alternative to total IL-6/IL-6R blockade. As disease progression increases trans-signalling through higher sIL-6R expression, early intervention in smouldering myeloma, before pathway amplification, may represent a more effective therapeutic strategy.

Keywords

Multiple myeloma; IL-6; sIL-6R; trans-signalling; sgp130; mesenchymal stromal cell

1. Introduction

Multiple myeloma (MM) is a haematological malignancy characterised by the clonal expansion of malignant plasma cells within the bone marrow (BM) [1]. Plasma cell disorders exist on a clinical spectrum, from the asymptomatic precursor state of smouldering multiple myeloma (SMM) to active MM [1, 2]. Unlike SMM, which is typically only monitored, active MM requires immediate systemic therapy [3]. Newly diagnosed patients with active MM typically receive induction therapy involving a combination of medications, which may include a proteasome inhibitor (e.g., bortezomib), an immunomodulatory agent (lenalidomide or thalidomide), an anti-CD38 monoclonal antibody, and the corticosteroid dexamethasone [4-6]. Despite significant therapeutic advances over recent decades, MM remains largely incurable, with most patients experiencing relapse and the development of treatment-resistant disease [7]. Disease persistence and progression are driven not only by the intrinsic properties of malignant plasma cells, but also by supportive interactions with the BM microenvironment [8]. This complex niche comprises multiple cellular components, including mesenchymal stromal cells (MSCs), osteoblasts, osteoclasts, endothelial cells, and immune cells, that can collectively provide pro-survival signals, promote drug resistance, and facilitate disease progression [9]. Among the diverse microenvironmental factors that support MM pathogenesis, the cytokine interleukin-6 (IL-6) has emerged as a central mediator of tumour–stroma cross-talk [10, 11]. IL-6 signals through three distinct mechanisms: classic signalling (cis-signalling), trans-signalling, and cluster signalling [12]. In classic signalling, IL-6 binds to the membrane-bound IL-6 receptor (mIL-6R; CD126), followed by the IL-6/mIL-6R complex associating with the ubiquitously expressed signal-transducing co-receptor glycoprotein 130 (gp130; CD130). Together they form a hexameric signalling platform that activates JAK–STAT3, MAPK, and PI3K–AKT intracellular pathways [13, 14]. In trans-signalling, IL-6 instead binds to the soluble IL-6 receptor (sIL-6R), generated by proteolytic shedding of mIL-6R by ADAM10 or ADAM17, or by alternative splicing of the IL-6R transcript [15-18]. The resulting IL-6/sIL-6R complex retains the ability to engage gp130 on cells that do not themselves express mIL-6R, thereby broadly extending IL-6 responsiveness across the BM microenvironment [19]. In cluster signalling, mIL-6R on one cell presents IL-6 in trans to gp130-expressing neighbouring cells via direct cell–cell contact [20].

Accurate quantification of IL-6, sIL-6R, and IL-6/sIL-6R complexes would be essential for dissecting IL-6 signalling biology in MM and for determining whether components of this pathway could serve as biomarkers of disease stage or therapeutic response. Previous studies have found that elevated sIL-6R levels do not always correlate with the amount of available free IL-6, highlighting that measuring a single component of a multifactorial signalling complex may be insufficient to fully capture pathway activity and its downstream biological impacts [21, 22]. Importantly, IL-6 signalling is compartmentalised, with free IL-6 and sIL-6R, as well as IL-6/sIL-6R complexes, differentially distributed across the BM and peripheral blood, so measurements from one compartment may not accurately reflect signalling activity in the other [23]. As trans-signalling is driven specifically by IL-6/sIL-6R complexes rather than by free IL-6, measuring total IL-6 alone is insufficient to determine the fraction of the cytokine that is biologically active. Distinguishing between free IL-6 and

complexed IL-6 is therefore necessary to accurately assess the extent of trans-signalling within a given compartment.

The main aim of this study was to determine the contributions of MSCs and MM cells, including primary material, to the IL-6 signalling machinery and how these change with disease progression. We also sought to elucidate the type of IL-6 signalling involved in the crosstalk between MSCs and MM cells, and its impact on cellular fates. Furthermore, we queried whether it is possible to measure the levels of the formed sIL-6R/IL-6 complex and to distinguish it from free sIL-6R and IL-6.

2. Methods

2.1. Cell Culture and Isolation of Patient-Derived Cells

2.1.1. Cell Culture of Human Cell Lines

The human myeloma cell lines, MM.1S, MM.1R, U266, and RPMI-8226, all purchased from Cytion Biosciences (Eppelheim, Germany), were cultured in RPMI-1640 medium containing 4.5 g/L D-Glucose, 2.383 g/L HEPES Buffer, 2 mM L-Glutamine, 1.5 g/L Sodium Bicarbonate and 110 mg/L Sodium Pyruvate (Thermo Fisher Scientific, Waltham, MA, USA), supplemented with 10% foetal bovine serum (FBS), 100 U/ml penicillin and 100 µg/ml streptomycin. MSCs, both adipose tissue-derived MSCs, purchased from AMSBio (Abingdon, United Kingdom), and BM-derived MSCs (BM-MSCs), purchased from Cytion Biosciences, were cultured in MesenPro RS Medium (Thermo Fisher Scientific), supplemented with 100 U/ml penicillin, 100 µg/ml streptomycin and 2 mM L-Glutamine. All cells were cultured in a humid incubator at 37°C and 5% CO_2.

2.1.2. Isolation of patient-derived MM cells and BM plasma

BM aspirates (4-7 ml) were obtained from patients at Colchester Hospital, following our protocol, which received favourable opinion from the Leeds East Research Ethics Committee and was approved by the Health Research Authority (IRAS Project ID: 324694, REC reference: 24/YH/0127). Eligible patients were those undergoing final assessments to confirm a diagnosis of either smouldering or active MM. All BM aspirates were processed via Ficoll-Paque density gradient centrifugation, following which the top layer of plasma was reserved for subsequent assays. The next layer, containing the BM mononuclear cells, was then isolated, and the cells were washed with phosphate-buffered saline (PBS) before the pellet was resuspended in sorting buffer (1% FBS in PBS) at a concentration of $1x10^8$ cells/ml. Biotin-tagged CD138 antibody (1:10 dilution; BioLegend, San Diego, CA, USA; Cat. No. 356535) and MojoSort Streptavidin Nanobeads (1:10 dilution; BioLegend; Cat. No. 480034) were then separated with the MojoSort magnet (Biolegend), following the manufacturer's instructions. These cells were used on the same day.

2.1.3. Isolation and Culture of BM-MSCs from MM patients (MM-MSCs)

After the MojoSort protocol, as above, all remaining CD138-negative cells were centrifuged and resuspended in 12 ml of MEM α Medium + GlutaMAX (Thermo Fisher Scientific), supplemented with 20% FBS, 100 U/ml penicillin and 100 µg/ml streptomycin. The cells were transferred to a T-75 cell culture flask and incubated at 37°C and 5% CO_2. No more than four days later, the medium was replaced to remove non-adherent cells. Medium replacements were continued twice weekly until sufficient MSCs were present to begin experiments, starting with staining for the cell-surface markers CD105, CD90, and CD45 to confirm the purity (>95%) of the MM-MSC culture.

2.2. Enzyme-linked immunosorbent assay (ELISA)

For ELISAs, cell culture supernatants were collected from MSCs or MM cells at the specified time points (48 h or 72 h). After centrifugation at 13,300 rpm for 15 min in a tabletop centrifuge, the supernatants were used in DuoSet ELISAs (Biotechne, Minneapolis, MN, USA) according to the manufacturer's instructions to determine IL-6 (Biotechne; Cat. No. DY206), sIL-6R (Biotechne; Cat. No. DY227) and IL-6/IL-6R complex levels (Biotechne; Cat. No. DY8139). For ELISAs of recombinant proteins, the proteins were mixed at the specified concentrations in reagent diluent and applied to DuoSet ELISAs (Biotechne). The recombinant proteins used were recombinant human IL-6 (rhIL-6) (Biotechne; Cat. No. 7270-IL/CF), sIL-6R (Biotechne; Cat. No. DY-277), gp130-Fc (Biotechne; Cat. No. 671-GP), chimaeric IL-6/sIL-6R protein (Biotechne; Cat. No. 8954-SR; referred to as Hyper-IL-6), IL-1α (Biotechne; Cat. No. 200-LA) and IL-1β (Biotechne; Cat. No. 201-LB). Hyper-IL-6 was used as the standard for IL-6/IL-6R complex ELISAs. For all ELISAs, the wash buffer used was 0.05% (v/v) Tween 20 in PBS, and the reagent diluent used was 1% Bovine Serum Albumin in PBS.

2.3. Cell surface marker stain

The MSCs or MM cells were harvested and incubated with APC-conjugated anti-human CD130 (gp130) antibody (2.5 µg/ml in PBS; BioLegend; Cat. No. 362005) or PE-conjugated anti-human IL-6R (10 µg/ml in PBS; BioLegend; Cat. No. 352803). APC-conjugated Mouse IgG2a, κ antibody (2.5 µg/ml in PBS; BioLegend; Cat. No. 400222) and PE-conjugated Mouse IgG1, κ antibody (10 µg/ml in PBS; BioLegend; Cat. No. 400113) were used as isotype control antibodies, respectively. After a 20 min incubation at 4°C, the cells were washed with PBS to remove excess antibody, then centrifuged before fixation in 4% paraformaldehyde. Once the cells were fixed, three readings of each sample were measured using the flow cytometer. The mean fluorescence intensity (MFI) ratio was calculated by dividing the MFI of the CD130 or IL-6R antibody stain by that of the corresponding isotype control.

2.4. Western blot

The cells were serum-starved overnight (16 h) in RPMI-1640 medium containing 0.2% FBS (MM.1R) or 0% FBS (MM.1S, U266 and RPMI-8226), or in 0.2% FBS low-glucose DMEM (MSC). The cells were then treated with 50 ng/ml rhIL-6 or 150 ng/ml Hyper-IL-6 protein for the specified time, then lysed in RIPA lysis buffer containing protease and phosphatase inhibitors. Once lysed, the protein concentration of each sample was determined using the Pierce BCA Protein Assay kit. Equal amounts of protein were then loaded onto a 10% sodium dodecyl-sulfate polyacrylamide gel. After separation via electrophoresis, the proteins were transferred to a polyvinylidene difluoride membrane. Following a 1 h block in 3% milk powder solution, the membranes were probed overnight in the corresponding primary antibody. Excess antibody was then washed off, with 0.1% Tween in Tris-buffered saline (TBST), before a 1 h incubation with the secondary antibody. After washing off the excess secondary antibody, the protein bands were visualised using a chemiluminescence imaging system with an enhanced chemiluminescence substrate (Thermo Fisher Scientific). β-tubulin (Elabscience, Houston, TX, USA; Cat. No. E-AB-40518) and total STAT3 (BioLegend;

Cat. No. 678001) antibodies were used as loading controls. Phospho-STAT3 antibodies against Ser727 (BioLegend; Cat. No. 669501) and Tyr705 (Cell Signaling Technology, Danvers, MA, USA ; Cat. No. 9131) were used to confirm cellular responsiveness to IL-6 and Hyper-IL-6. Horseradish peroxidase-linked anti-mouse IgG (Cell Signaling Technology; Cat. No. 7076) and anti-rabbit IgG (Cell Signaling Technology; Cat. No. 7074) antibodies were used as secondary antibodies. All antibodies were diluted at either 1:500 (anti-STAT3) or 1:1000 (all other antibodies) in TBST containing 3% milk powder. Where necessary due to overlapping molecular weights, proteins were analysed on separate membranes, with β-tubulin confirming equal protein loading on each membrane.

2.5. DNA Hypodiploidy Assay

To monitor cell death responses, MM.1S cells were plated at a density of $5x10^4$ cells/well in 48-well plates (500 µl total volume). They were given 24 h to adhere to the plate before being treated with dexamethasone (100 µM; Selleck Chemicals, Houston, TX, USA; Cat. No. S3124), in the presence or absence of rhIL-6, Hyper-IL-6 protein, or MSC-conditioned supernatant (MSC SN; 100 µl; collected after ≥72 h from confluent MSC cultures; untreated or preincubated for 20 min with soluble gp130 (sgp130; 5 µg/ml; Cambridge Bioscience, Cambridge, UK; Cat. No. 10974-H03H-20) or vehicle control. Separately, MM.1S cells were pre-incubated for 30 min with Tocilizumab (10 µg/ml; Cambridge Bioscience; Cat. No. 68131-H001-500), or human IgG1, κ (10 µg/ml; BioLegend; Cat. No. 403501), as an isotype control for Tocilizumab, prior to treatment with MSC SN (100 µl) and dexamethasone (100 µM). In all cases, 48 h after treatment, the percentage of hypodiploid cells was measured as previously described [24]. Briefly, the cells were harvested and, following centrifugation, the cell pellet was resuspended in a hypotonic fluorochrome solution containing 0.1% (w/v) sodium citrate, 0.1% (v/v) Triton-X100 and 20 µg/ml propidium iodide. The cells were then analysed by flow cytometry, and the percentage of hypodiploid cells was recorded.

2.6. Reverse Transcription and PCR

Total RNA was isolated from MSCs and MM cells using the Monarch Total RNA Miniprep Kit (New England Biolabs, Ipswich, MA, USA) according to the manufacturer's protocol, including the on-column DNase I digestion step to eliminate genomic DNA contamination. Equal quantities of RNA (200 ng) were reverse-transcribed into complementary DNA (cDNA) using the LunaScript RT SuperMix Kit (New England Biolabs) in accordance with the manufacturer's instructions. PCR amplification was subsequently performed using DreamTaq Green PCR Master Mix (2×) (Thermo Fisher Scientific) in a total reaction volume of 20 µl containing 2 µl cDNA template and 0.5 µM IL-6R forward (5'-CTCAGTGTCACCTGGCAAGA) and reverse (5'-GTGGGGAGATGAGAGGAACA) primers. Thermal cycling conditions were used as published by Oh et al [25]. PCR products were resolved by 2% agarose gel electrophoresis in 1× TAE buffer, stained with SYBR Safe (Thermo Fisher Scientific), and visualised under UV illumination. PCR reactions were purified (GenElute™ PCR Clean-Up Kit; Merck, Darmstadt, Germany; Cat. No. NA-1020) and sent for Sanger sequencing (Eurofins Genomics, Ebersberg, Germany)

2.7. Statistical Analysis

Experimental data are presented as the mean ± the standard error of the mean (SEM). Differences between groups were analysed using a one-way analysis of variance (ANOVA) unless otherwise stated. For experiments involving patient-derived cells, statistical significance between groups was assessed using a two-tailed Mann-Whitney U test. A p-value>0.05 was considered not significant, whereas *p≤0.05, **p≤0.01, and ***p≤0.001 were considered statistically significant. Samples were measured in triplicate, and experiments were repeated a total of three times independently unless otherwise stated. Technical replicates were averaged prior to statistical analysis, and statistical tests were performed using the mean from each independent experiment.

3. Results

3.1. MSCs and MM cells differentially contribute to the IL-6 signalling axis

IL-6 signalling within the MM BM niche is inherently complex, arising from the combined, potentially distinct contributions of various cell types, including MSCs and malignant plasma cells. To identify the cellular sources of IL-6 and sIL-6R within the MM microenvironment, we quantified secretion of these two factors by MSCs and MM cell lines, respectively. Healthy MSCs (from here on referred to as MSCs) secreted robust levels of IL-6 under normal growth conditions, whereas MM cell lines showed undetectable levels of IL-6 under standard culture conditions (Fig. 1A). Exposure of MSCs and MM cells to the pro-inflammatory stimuli IL-1α (Fig. 1B) and IL-1β (Fig. 1C) led to a dose-dependent increase in IL-6 secretion, plateauing at around 35 ng/ml, in MSCs but not MM cells. These results demonstrate that inflammatory cues present in the tumour microenvironment (TME) can further amplify stromal IL-6 production. In order to determine whether cells possess the necessary cognate receptor, we assessed mIL-6R expression on MSCs (Fig. 1D) and MM cells (Fig. 1E). We found no detectable levels of mIL-6R on MSCs, whereas all four MM cell lines exhibited robust expression. As IL-6R can also occur as a soluble version, we assessed sIL-6R in cellular supernatants and found that MM cell lines released readily measurable levels of sIL-6R, whereas MSCs did not (Fig. 1F). As sIL-6R can be generated via alternative mRNA splicing or proteolytic cleavage of initially mIL-6R, we conducted RT-PCR analysis followed by PCR amplicon sequencing. We found no evidence of alternative transcripts lacking exon 9 that could lead to sIL-6R (Fig. 1G and Supplementary Fig. 1) [17, 18, 25, 26]. Therefore, limited proteolytic processing of mIL-6R seems to be the main contributor to sIL-6R in the supernatants of MM cell lines. Overall, these data demonstrate a compartmentalised distribution of IL-6 signalling components, in which MSCs provide the ligand, IL-6, and MM cells provide the soluble receptor.

3.2. MM cells respond to IL-6 signalling with STAT3 phosphorylation

Having found that MSCs express IL-6 and MM cells shed sIL-6R that together can lead to IL6/sIL6R complex formation and functional IL-6 trans-signalling, we next investigated whether MM cells and MSCs express membrane-bound gp130 (mgp130). The signal-

transducing receptor subunit gp130 is required for recognition of the IL-6/sIL-6R complex and for activation of downstream signalling, including the JAK/STAT pathway via the trans-signalling mode [27]. Flow cytometric surface stain analysis revealed expression of mgp130 on all four MM cell lines investigated (Fig. 2A). Likewise, three separate batches of MSCs all displayed mgp130 expression (Fig. 2B), albeit at varying levels, indicating that both MM cells and MSCs are principally competent to respond to IL-6/sIL-6R complexes. To demonstrate functional IL-6 responsiveness, we next examined STAT3 serine and tyrosine phosphorylation in the MM cell lines following stimulation with rhIL-6. Three out of the four cell lines (MM.1S, MM.1R and RPMI-8226) showed very low basal levels of phosphoserine-STAT3 (Ser727) and demonstrated significant induction of this phosphorylation following IL-6 stimulation (Fig. 2C). The U266 cell line exhibited high constitutive STAT3 phosphorylation at Ser727 that did not increase further upon addition of rhIL-6 (Fig. 2C). Measuring tyrosine phosphorylation of STAT3 (Tyr705) revealed a slightly different picture. In this case all four MM cell lines, including U266 cells, responded robustly with induced Tyr 705 phosphorylation (Fig. 2C). Owing to their lack of mIL-6R, MSCs did not respond to rh-IL6 with induced Ser727 or Tyr705 phosphorylation while showing elevated basal Ser727 phosphorylation levels (Fig. 2D). Since MSCs lack both mIL-6R and sIL-6R to form the active IL-6/sIL-6R complex, we stimulated them with Hyper-IL-6 [28]. This experiment revealed that treated MSCs exhibited induced Tyr705 phosphorylation, whereas Ser727 phosphorylation remained unchanged (Fig. 2E). MM cells responded similarly to Hyper-IL-6 as to rhIL-6, except that two Tyr705 STAT3 bands were observed in the immunoblot after Hyper-IL-6 treatment. This is possibly caused by Hyper-IL-6 affording tyrosine phosphorylation of more than one STAT3 isoform or additional post-translational modifications [29, 30] (Fig. 2F). These results indicate that MSCs can only potentially respond to IL-6 trans-signalling, whereas MM cells are principally able to transduce signals via both cis and trans pathways.

3.3. IL-6 trans-signalling protects MM cells from dexamethasone-induced cell death

We then set out to determine whether IL-6 signalling affects MM cells and whether it confers survival benefits to them. To investigate this, we treated MM.1S cells with dexamethasone in the presence of rhIL-6. Unlike cells treated solely with dexamethasone, those co-treated with rhIL-6 showed significant protection against apoptosis (Fig. 3A). Next, we examined whether IL-6-containing MSC SN could shield MM.1S cells from dexamethasone-induced cell death. After adding the supernatants from MSCs to dexamethasone-treated MM cells, we also observed notable protection from cell death induced by dexamethasone (Fig. 3B). To assess whether this protection is mediated by IL-6 trans-signalling or canonical signalling, we added Hyper-IL-6 to MM.1S cells and measured apoptosis in response to dexamethasone. This chimaeric protein can bind only to gp130 and acts via the trans-signalling mechanism. We found that the IL-6/sIL-6R protein protected MM cells from the effects of dexamethasone, demonstrating that IL-6 trans-signalling can provide protection against steroid-induced cell death (Fig. 3C). To further dissect the roles of cis- and trans-signalling afforded by MSC SN we utilised the anti-IL-6R antibody Tocilizumab. Tocilizumab can block both types of signalling. Mixing the antibody with MM cells that were subsequently treated

with MSC SN and dexamethasone revealed that Tocilizumab could block the MSC SN mediated protection (Fig. 3D). To assess the role of trans-signalling in this protection, we added sgp130 to the MSC SN and applied the mix to MM cells [31-33]. The addition of sgp130 blocked the protection from dexamethasone-triggered apoptosis to almost the same level as Tocilizumab (Fig. 3E), indicating that trans-signalling is the predominant mediator of protection from dexamethasone-induced cell death.

3.4. The IL-6 signalling axis is amplified with disease progression

Next, we wanted to know whether our findings would also apply to primary cells derived from the TME of MM patients. For this, we isolated patient-derived MM-MSCs and CD138-positive malignant plasma cells from patients with smouldering and newly diagnosed active MM. Flow-cytometric surface analysis of gp130 revealed that gp130 was constitutively expressed on the surface of MM-MSCs irrespective of disease stage (Fig. 4A). Quantification of this expression confirmed gp130 positivity in all MM-MSCs tested but also revealed a high degree of inter-patient heterogeneity, with expression levels varying considerably between individuals (Fig. 4B). However, no significant correlation was found between disease stage and gp130 expression (Fig. 4B). When we examined IL-6 levels secreted by MM-MSCs, we could not find a difference between healthy MSCs and MM-MSCs from patients with smouldering disease (Supplementary Fig. 2). MM-MSCs from patients with active MM, however, showed a significant increase in IL-6 levels (Fig. 4C). Subsequently, we evaluated sIL-6R release by patient-derived CD138-positive MM cells. We observed that sIL-6R was also associated with disease stage. Cells from patients with active disease released significantly more sIL-6R than MM cells from patients with smouldering disease. (Fig. 4D). IL-6 production remained low in these cells from both patient groups (Fig. 4E). Notably, these disease-stage-specific differences were not observed in patient BM plasma, as we found no differences in IL-6 levels in this fluid between SMM and active MM (Fig. 4F). This suggests that while IL-6 and sIL-6R show promise as potential biomarkers, the cellular compartmental site of measurement is a critical determinant of their diagnostic utility.

3.5. IL-6 ELISA fails to differentiate between free and complexed IL-6

While measuring free IL-6 and sIL-6R provided useful information about disease stage, we thought determining the levels of the active IL-6/sIL-6R complex formed from these components could deliver an even better understanding of the extent of IL-6 trans-signalling capacity. First, we tested the IL-6 ELISA to determine whether its ability to quantify IL-6 would be impacted by sgp130 or sIL-6R. Our results show that the addition of sIL-6R, sgp130, or a combination of both did not impair or alter the ability of the ELISA to detect IL-6 (Fig. 5A), indicating that complex formation between these signalling components does not interfere with the ELISA. To test this further, we applied Hyper-IL-6 to the IL-6 ELISA and found that it also detected the IL-6 part in the chimaeric fusion protein (Fig. 5B). Combining the chimaeric protein with rhIL-6, in the presence or absence of sgp130, also did not affect the ability of the IL-6 ELISA to detect all IL-6, regardless of its complexed state (Fig. 5B). Next, we assessed the use of the only widely cited commercial kit specifically designed for IL-6/sIL-6R complexes to determine the extent of complex formation upon mixing IL-6 and sIL-

6R at the same concentrations used above. Surprisingly, only Hyper-IL-6 was robustly detected in this ELISA, whilst the formed IL-6/sIL-6R complex was not (Fig. 5C). In addition, rhIL-6 and sIL-6R alone failed to produce any detectable signal (Fig. 5C). Furthermore, adding sgp130 to the IL-6/sIL-6R mix did not affect the detection capability of the ELISA (Fig. 5C). The addition of IL-6, alone or alongside sgp130, to the Hyper-IL-6 protein did not impede or enhance its detection (Fig. 5D). These results demonstrate that the ELISA can accurately detect the IL-6/sIL-6R chimaeric fusion protein (Hyper-IL-6). However, at moderate concentrations of IL-6 and sIL-6R it is not sensitive enough for measuring active, naturally formed IL-6/sIL-6R complex. To test the ELISA further, we used supernatants from MM cells that produced the highest levels of sIL-6R (U266 cells) combined with supernatants from IL-1α-stimulated MSCs. Here we found that the IL-6/sIL-6R complex can be detected, albeit at low concentrations. However, the measured complex concentrations were far below the calculated theoretical values, as previously reported (Figure 5E) [34]. Thus, while the use of this ELISA remains challenging at lower concentrations of IL-6 and sIL-6R, it becomes useful in inflammatory settings that give rise to higher IL-6 levels, as in sepsis, arthritis or the TME.

4. Discussion

The present study demonstrates that sIL-6R release by primary CD138-positive MM cells is significantly associated with disease stage. Cells derived from patients with newly diagnosed active MM released approximately twice as much sIL-6R as those from patients with smouldering disease. This finding suggests that sIL-6R production is dynamically regulated during MM progression and that elevated sIL-6R release is a hallmark of biologically active disease. The observation is consistent with previous research demonstrating that serum sIL-6R levels correlate with MM disease stage [35-37]. Importantly, however, in contrast to those studies, which predominantly rely on serum measurements that may simply reflect the overall cancer burden, our approach revealed that individual MM cells from active disease intrinsically secrete greater quantities of sIL-6R than those from smouldering stages. This cell-level distinction underscores the potential of sIL-6R release as a biomarker for disease staging and highlights a biologically meaningful shift in cytokine signalling capacity as MM transitions from smouldering to active disease.

Complementing these findings, analysis of cellular IL-6 production sites within the BM niche revealed that MSCs, rather than MM cells, are the dominant source of IL-6. MM cell lines and primary MM cells produced minimal or undetectable IL-6, suggesting that the malignant compartment does not represent a significant autocrine source of this cytokine. The role of stromal cells as the principal cytokine source is consistent with earlier reports identifying BM-MSCs as the predominant IL-6 producers within the MM niche [8, 38]. Our data extend these findings by demonstrating that MSCs not only constitutively secrete IL-6 but also respond robustly to inflammatory stimuli, thereby further amplifying their IL-6 output. This inducibility is particularly relevant in the context of active MM, where the inflammatory milieu of the BM is known to be markedly elevated [39], suggesting that stromal IL-6 production is not static but dynamically reinforced by the evolving TME. In addition, we found that IL-6 production by MM-MSCs correlates with disease stage, whereas corresponding IL-6 levels in plasma do not. Notably, the increased IL-6 levels were detected in cultured MM-MSCs that had gone through a number of passages. Thus, the regulation of IL-6 production must have changed in a more sustained, non-reversible manner during disease progression in these cells. Understanding the underlying mechanisms could reveal new therapeutic intervention points.

The convergence of MSC-derived IL-6 and MM cell-derived sIL-6R within the BM niche creates the conditions for the assembly of active IL-6/sIL-6R complexes capable of engaging gp130-mediated trans-signalling. Classic IL-6 signalling is restricted to a defined subset of cells expressing mIL-6R. In contrast, trans-signalling through gp130 broadens IL-6 responsiveness to potentially all cells within the microenvironment [12, 19] that display mgp130 on their surface. Therefore, determining the levels of the active complex, rather than the individual constituents, would be important. Our attempts to measure the levels of active IL-6/sIL-6R complex in mixes of free rhIL-6 and sIL-6R failed because the commercially available ELISA was not sensitive enough for this purpose. We found that the assay could detect only recombinant Hyper-IL-6 protein, not naturally formed IL-6/sIL-6R complexes at lower levels. This is most likely attributable to the insufficient concentration of

physiologically occurring IL-6/sIL-6R under normal and healthy conditions. However, while this ELISA presents limitations at physiologically low concentrations of IL-6 and sIL-6R, it demonstrates meaningful utility in pathological states characterised by substantially elevated cytokine levels. Such conditions include sepsis, in which circulating IL-6 can reach nanogram-per-millilitre concentrations, as well as rheumatoid arthritis and the TME, where sustained cytokine production by activated immune cells and MSCs generate a robustly detectable signal [40-44]. In these contexts, the assay may serve as a practical tool for disease monitoring, patient stratification, or evaluation of therapeutic interventions targeting the IL-6/sIL-6R signalling axis.

Our data provide strong evidence that the well-established protective effect of stromal-derived IL-6 against dexamethasone-induced apoptosis in MM cells is specifically mediated through the IL-6 trans-signalling mechanism. While prior studies have demonstrated that IL-6 derived from BM-MSCs can protect MM cells from glucocorticoid-induced apoptosis, the precise signalling mechanism responsible for this protection had remained unresolved [45, 46]. We demonstrated that Hyper-IL-6 recapitulated dexamethasone resistance induced by MSC-conditioned medium in MM.1S cells, directly implicating trans-signalling as the predominant mechanism. This distinction has considerable biological and therapeutic relevance. It implies that clinically observed glucocorticoid resistance driven by the BM microenvironment is not contingent on mIL-6R expression on MM cells but instead operates through the ubiquitously expressed gp130, rendering virtually all MM cells susceptible to this stromal mechanism, irrespective of their mIL-6R status. This conclusion is supported by the fact that recombinant sgp130-Fc markedly reversed MSC SN-mediated protection of MM cells from dexamethasone-induced apoptosis. This effect was comparable to that of Tocilizumab, supporting the notion that trans-signalling is the main mechanism involved, while not entirely excluding a contributory role of cis-signalling. Indeed, cis-signalling remains possible, as MM cells display mIL-6R, before being proteolytically cleaved to sIL-6R.

Total IL-6 signalling inhibition with IL-6 antibodies (e.g. Siltuximab) or IL-6R antibodies (e.g. Tocilizumab) in anti-cancer approaches has demonstrated preclinical activity [12, 47], yet clinical trials have yielded modest results to date [48]. In MM trials, Siltuximab showed encouraging results, but it was also associated with increased haematologic toxicity and infection rates [49, 50]. These findings suggest that the adverse effects of broad IL-6 blockade stem, at least in part, from the inadvertent suppression of beneficial classical IL-6 signalling. Selective inhibition of trans-signalling via sgp130-Fc, now advanced into clinical trials as Olamkicept, preserves this homeostatic arm while blocking the pathological IL-6/sIL-6R complex, and therefore warrants investigation as a more targeted strategy with an improved benefit-to-risk profile in some diseases including MM [12].

5. Conclusions

In conclusion, using primary patient-derived MSCs and CD138-positive malignant plasma cells isolated from patients with both smouldering and active MM, we demonstrate that IL-6 signalling within the MM BM-niche is functionally compartmentalised. MSCs are the

principal source of IL-6, whilst myeloma cells are the main source of sIL-6R, establishing a paracrine IL-6 trans-signalling axis in which each cell type contributes a distinct and non-redundant component. The magnitude of this axis is not fixed but amplifies with disease progression: sIL-6R release by patient-derived MM cells is significantly greater in active disease than in SMM, identifying sIL-6R as a marker of biologically active disease, mirrored by elevated IL-6 output from MSCs in advanced-stage patients. Functionally, we establish that trans-signalling through gp130, and not classic mIL-6R-dependent signalling, is the predominant mechanism by which stromal-derived IL-6 protects myeloma cells from treatment-induced apoptosis. Collectively, these findings reframe the IL-6 axis in MM as a cooperative, stage-dependent, and compartmentalised circuit, and suggest that selective blockade of trans-signalling, and early therapeutic intervention in SMM before pathway amplification is established, may represent more effective strategies than current broad anti-IL-6 approaches.

Acknowledgements

We would like to acknowledge the Colchester Haematology R&D team for their valuable support. PEB is funded by the East Suffolk and North Essex NHS Foundation Trust.

CRediT authorship contribution statement

Phoebe Elizabeth Blair: Writing – original draft, Writing – review & editing, Investigation, Methodology, Visualisation, Formal analysis, Validation, Data curation. **Tianyuan Chu:** Writing – review & editing, Investigation, Formal analysis. **Andrew Robinson:** Writing – review & editing, Conceptualisation, Resources. **Khalid Saja:** Writing – review & editing, Funding acquisition, Conceptualisation, Resources. **Stuart Rushworth:** Writing – review & editing, Conceptualisation, Resources. **Ralf Zwacka:** Writing – original draft, Writing – review & editing, Supervision, Formal analysis, Methodology, Conceptualisation. **Andrea Mohr:** Writing – review & editing, Writing – original draft, Visualisation, Validation, Supervision, Project administration, Methodology, Funding acquisition, Formal analysis, Conceptualisation.

Declaration of Interest Statement

The authors report there are no competing interests to declare.

Data availability statement

The data supporting the findings of this study can be obtained upon reasonable request. Requests should be made to the corresponding authors.

Figure legends

Fig. 1. MSCs and MM cells differentially contribute to the IL-6 signalling axis

(A) Human MM cell lines and MSCs were plated at 5 x 10^4 cells/well and 1 × 10^4 cells/well, respectively, in 48-well plates (500 µl total volume). After 72 h, supernatants were collected, and IL-6 levels were quantified by ELISA. Data represent mean ± SEM (n=3). (B) Human MSCs and MM cell lines were plated at 1 × 10^4 cells/well or 5 x 10^4 cells/well, respectively, in 48-well plates (500 µl total volume) and stimulated with the indicated amounts of IL-1α. After 72 h, supernatants were collected, and IL-6 levels were quantified by ELISA. IL-6 levels are shown as mean pg/ml ± SEM (n=3). (C) Human MSCs and MM cell lines were plated at 1 × 10^4 cells/well or 5 x 10^4 cells/well, respectively, in 48-well plates (500 µl total volume) and stimulated with the indicated amounts of IL-1β. After 72 h, supernatants were collected, and IL-6 levels were quantified by ELISA. IL-6 levels are shown as mean pg/ml ± SEM (n=3). (D) Flow cytometric analysis of IL-6R surface expression on MSCs (red). The respective isotype control is shown in black. A representative histogram is shown, with the mean MFI ratio (n=3 technical replicates) indicated in the top-right corner. (E) Flow cytometric analyses of IL-6R surface expression on MM cell lines (red). The respective isotype controls are shown in black. Representative histograms are shown with the mean MFI ratio (n=3 technical replicates) indicated in the top-right corners. (F) Supernatants from (A) were analysed for sIL-6R by ELISA. Data represent mean ± SEM (n=3). (G) RT-PCR analysis of IL-6R transcripts in MM cell lines and MSCs.

Fig. 2. MM cells respond to IL-6 signalling with STAT3 phosphorylation

(A) Flow cytometric analysis of gp130 expression on human MM cell lines (red). The respective isotype control is shown in black. Representative histograms are shown with the mean MFI ratio (n=3 technical replicates) indicated in the top-right corner of each histogram. (B) gp130 expression on MSCs from three independent healthy donors was analysed as in (A), with the mean MFI ratio (n=3 technical replicates) indicated in the top-right corner of each histogram. (C) Western blot analysis of STAT3 phosphorylation in FBS-starved human MM cell lines stimulated with rhIL-6 (50 ng/ml) for the time points indicated. Total STAT3 and β-tubulin served as loading controls. (D) Western blot analysis of STAT3 phosphorylation in FBS-starved MSCs stimulated with rhIL-6 (50 ng/ml) for the time points indicated. Total STAT3 and β-tubulin served as loading controls. (E) Western blot analysis of STAT3 phosphorylation in FBS-starved MSCs stimulated with Hyper-IL-6 (150 ng/ml) for the time points indicated. Total STAT3 and β-tubulin served as loading controls. (F) Western blot analysis of STAT3 phosphorylation in FBS-starved MM.1S cells stimulated with Hyper-IL-6 (150 ng/ml) for the time points indicated. Total STAT3 and β-tubulin served as loading controls.

Fig. 3. IL-6 trans-signalling protects MM cells from dexamethasone-induced cell death

(A) Quantification of hypodiploid MM cells following treatment with rhIL-6 (50 ng/ml) in the presence or absence of dexamethasone (100 μM). Data represent mean ± SEM from three independent experiments. (B) Effect of MSC SN (100 μl) on dexamethasone-induced cell death in MM.1S cells. Hypodiploid cells were quantified as in (A). (C) Quantification of hypodiploid MM.1S cells following stimulation with Hyper-IL-6 (50 ng/ml) in the presence or absence of dexamethasone (100 μM). Data represent mean ± SEM from three independent experiments. (D) MM.1S cells were treated with dexamethasone (100 μM) alone or in combination with MSC SN (100 μl), anti-IL-6R antibody/Tocilizumab (10 μg/ml), or isotype control for Tocilizumab (10 μg/ml), and hypodiploid cells were quantified as above. (E) MM.1S cells were treated with dexamethasone (100 μM) alone or in combination with MSC SN (100 μl), sgp130 (5 μg/ml), or vehicle control (PBS), and hypodiploid cells were quantified as above.

Fig. 4. The IL-6 signalling axis is amplified with disease progression

(A) Flow cytometric analysis of gp130 expression on patient-derived MM-MSCs (red). The respective isotype control is shown in black. Representative histograms are shown for MM-MSCs from a patient with SMM and from a patient with active disease, with the mean MFI ratio (n=3 technical replicates) indicated in the top-right corner of each histogram. (B) Quantification of gp130 MFI ratios in patient-derived MM-MSCs. Each data point represents the mean MFI ratio (n=3 technical replicates) per sample. Black bars indicate patient group means (n=5 per group). (C) MM-MSCs were cultured at 0.2×10^4 cells/well in 96-well plates (200 μl total volume) for 72 h. Supernatants were analysed for IL-6 by ELISA (n=5 SMM; n=5 active MM). (D) CD138-positive cells isolated from the BM of patients with smouldering or active MM were cultured at 1×10^4 cells/well in 48-well plates (400 μl total volume) for 48 h. Supernatants were analysed for sIL-6R by ELISA (n=5 SMM; n=5 active MM). (E) CD138-positive cells isolated from the BM of patients with smouldering or active MM were cultured as in (D). Supernatants were analysed for IL-6 by ELISA (n=5 SMM; n=5 active MM). (F) BM plasma from patients with SMM and active MM was analysed for IL-6 by ELISA (n=5 SMM; n=5 active MM).

Fig. 5. IL-6 ELISA fails to differentiate between free and complexed IL-6

(A) rhIL-6 (125 pg/ml), sIL-6R (230 pg/ml), and sgp130 (570 pg/ml) were incubated in indicated combinations for 20 min and analysed by IL-6 ELISA. Data represent mean ± SEM (n=3). (B) rhIL-6 (125 pg/ml), Hyper-IL-6 (355 pg/ml), and sgp130 (570 pg/ml) were analysed as in (A). (C). Hyper-IL-6 (355 pg/ml), rhIL-6 (125 pg/ml), sIL-6R (230 pg/ml) and sgp130 (570 pg/ml) were incubated in indicated combinations for 20 min and analysed by IL-6/sIL-6R complex ELISA. Data represent mean ± SEM (n=3). (D) Hyper-IL-6 (355 pg/ml), rhIL-6 (125 pg/ml) and sgp130 (570 pg/ml) were analysed as in (C). (E) Supernatants from

U266 cells (10 μl) were mixed with supernatants from either untreated (10 μl) or IL-1α-treated (4 ng) MSCs (10 μl), incubated for 1 h and analysed by IL-6/sIL-6R complex ELISA. Data represent mean (subtracted by the background values) ± SEM (n=3).

Declaration of generative AI and AI-assisted technologies in the manuscript preparation process

During the preparation of this work, the authors used Grammarly to check language, grammar, and spelling. Furthermore, the authors used SciSpace to create the graphical abstract. After using these tools, the authors reviewed and edited the content as needed and take full responsibility for the content of the published article.

References

[1] S.V. Rajkumar, M.A. Dimopoulos, A. Palumbo, J. Blade, G. Merlini, M.-V. Mateos, S. Kumar, J. Hillengass, E. Kastritis, P. Richardson, O. Landgren, B. Paiva, A. Dispenzieri, B. Weiss, X. LeLeu, S. Zweegman, S. Lonial, L. Rosinol, E. Zamagni, S. Jagannath, O. Sezer, S.Y. Kristinsson, J. Caers, S.Z. Usmani, J.J. Lahuerta, H.E. Johnsen, M. Beksac, M. Cavo, H. Goldschmidt, E. Terpos, R.A. Kyle, K.C. Anderson, B.G.M. Durie, J.F.S. Miguel, International Myeloma Working Group updated criteria for the diagnosis of multiple myeloma, The Lancet Oncology 15(12) (2014) e538–e548.

[2] S.V. Rajkumar, Multiple myeloma: 2024 update on diagnosis, risk-stratification, and management, American Journal of Hematology 99(9) (2024) 1802–1824.

[3] T. Schmidt, Z. Gahvari, N.S. Callander, SOHO State of the Art Updates and Next Questions: Diagnosis and Management of Monoclonal Gammopathy of Undetermined Significance and Smoldering Multiple Myeloma, Clinical Lymphoma Myeloma and Leukemia 24(10) (2024) 653–664.

[4] R. Della Pepa, S. Palmieri, S. Rocco, N. Pugliese, A. Leone, S. Avilia, M. Barone, R. Rosamilio, F. Trastulli, D. De Novellis, R. Fontana, B. Serio, D. Morini, L. Esposito, L. De Fazio, R. Spisso, C. Selleri, C. Califano, A. Picardi, M. Annunziata, F. Pane, Impact of Dara-VTD induction therapy on stem cell mobilization outcomes in newly diagnosed multiple myeloma patients undergoing autologous stem cell transplantation: a multicenter study, Annals of Hematology 104(10) (2025) 5371–5378.

[5] T. Facon, M.A. Dimopoulos, X.P. Leleu, M. Beksac, L. Pour, R. Hájek, Z. Liu, J. Minarik, P. Moreau, J. Romejko-Jarosinska, I. Spicka, V.I. Vorobyev, B. Besemer, T. Ishida, W. Janowski, S. Kalayoglu-Besisik, G. Parmar, P. Robak, E. Zamagni, H. Goldschmidt, T.G. Martin, S. Manier, M. Mohty, C. Oprea, M.F. Brégeault, S. Macé, C. Berthou, D. Bregman, Z. Klippel, R.Z. Orlowski, Isatuximab, Bortezomib, Lenalidomide, and Dexamethasone for Multiple Myeloma, New England Journal of Medicine 391(17) (2024) 1597–1609.

[6] P. Sonneveld, M.A. Dimopoulos, M. Boccadoro, H. Quach, P.J. Ho, M. Beksac, C. Hulin, E. Antonioli, X. Leleu, S. Mangiacavalli, A. Perrot, M. Cavo, A. Belotti, A. Broijl, F. Gay, R. Mina, I.S. Nijhof, N. van de Donk, E. Katodritou, F. Schjesvold, A. Sureda Balari, L. Rosiñol, M. Delforge, W. Roeloffzen, T. Silzle, A. Vangsted, H. Einsele, A. Spencer, R. Hajek, A. Jurczyszyn, S. Lonergan, T. Ahmadi, Y. Liu, J. Wang, D. Vieyra, E.M.J. van Brummelen, V. Vanquickelberghe, A. Sitthi-Amorn, C.J. de Boer, R. Carson, P. Rodriguez-Otero, J. Bladé, P. Moreau, Daratumumab, Bortezomib, Lenalidomide, and Dexamethasone for Multiple Myeloma, New England Journal of Medicine 390(4) (2024) 301–313.

[7] A. Palumbo, K. Anderson, Multiple myeloma, New England Journal of Medicine 364(11) (2011) 1046–1060.

[8] T. Hideshima, C. Mitsiades, G. Tonon, P.G. Richardson, K.C. Anderson, Understanding multiple myeloma pathogenesis in the bone marrow to identify new therapeutic targets, Nature Reviews Cancer 7(8) (2007) 585–598.

[9] G. Bianchi, N.C. Munshi, Pathogenesis beyond the cancer clone(s) in multiple myeloma, Blood 125(20) (2015) 3049–3058.

[10] M. Kawano, T. Hirano, T. Matsuda, T. Taga, Y. Horii, K. Iwato, H. Asaoku, B. Tang, O. Tanaka, H. Fujiwara, T. Kishimoto, Autocrine generation and requirement of BSF-2/IL-6 for human multiple myelomas, Nature 332(6159) (1988) 83–85.

[11] B. Klein, X.-G. Zhang, M. Jourdan, J. Content, F. Houssiau, L. Aarden, M. Piechaczyk, R. Bataille, Paracrine rather than autocrine regulation of myeloma-cell growth and differentiation by interleukin-6, Blood 73(2) (1989) 517–526.

[12] S. Rose-John, B.J. Jenkins, C. Garbers, J.M. Moll, J. Scheller, Targeting IL-6 trans-signalling: past, present and future prospects, Nature Reviews Immunology 23(10) (2023) 666–681.

[13] M. Hibi, M. Murakami, M. Saito, T. Hirano, T. Taga, T. Kishimoto, Molecular cloning and expression of an IL-6 signal transducer, gp130, Cell 63(6) (1990) 1149–1157.

[14] T. Kishimoto, T. Taga, S. Akira, Cytokine signal transduction, Cell 76(2) (1994) 253–262.

[15] A. Chalaris, C. Garbers, B. Rabe, S. Rose-John, J. Scheller, The soluble Interleukin 6 receptor: generation and role in inflammation and cancer, European Journal of Cell Biology 90(6-7) (2011) 484–494.

[16] S. Rose-John, P.C. Heinrich, Soluble receptors for cytokines and growth factors: generation and biological function, Biochemical Journal 300(2) (1994) 281–290.

[17] J.A. Lust, K.A. Donovan, M.P. Kline, P.R. Greipp, R.A. Kyle, N.J. Maihle, Isolation of an mRNA encoding a soluble form of the human interleukin-6 receptor, Cytokine 4(2) (1992) 96–100.

[18] N. Schumacher, D. Meyer, A. Mauermann, J. von der Heyde, J. Wolf, J. Schwarz, K. Knittler, G. Murphy, M. Michalek, C. Garbers, J.W. Bartsch, S. Guo, B. Schacher, P. Eickholz, A. Chalaris, S. Rose-John, B. Rabe, Shedding of Endogenous Interleukin-6 Receptor (IL-6R) Is Governed by A Disintegrin and Metalloproteinase (ADAM) Proteases while a Full-length IL-6R Isoform Localizes to Circulating Microvesicles, J Biol Chem 290(43) (2015) 26059–26071.

[19] S. Rose-John, IL-6 trans-signaling via the soluble IL-6 receptor: importance for the pro-inflammatory activities of IL-6, International Journal of Biological Sciences 8(9) (2012) 1237–1247.

[20] S. Heink, N. Yogev, C. Garbers, M. Herwerth, L. Aly, C. Gasperi, V. Husterer, A.L. Croxford, K. Möller-Hackbarth, H.S. Bartsch, K. Sotlar, S. Krebs, T. Regen, H. Blum, B. Hemmer, T. Misgeld, T.F. Wunderlich, J. Hidalgo, M. Oukka, S. Rose-John, J. Scheller, T. Korn, A. Waisman, H. Wekerle, H.W. Mittrücker, M. Lohoff, B. Becher, Trans-presentation of IL-6 by dendritic cells is required for the priming of pathogenic TH17 cells, Nature Immunology 18(1) (2017) 74–85.

[21] K. Pulkki, T.-T. Pelliniemi, A. Rajamäki, A. Tienhaara, M. Laakso, R. Lahtinen, Soluble interleukin-6 receptor as a prognostic factor in multiple myeloma. Finnish Leukaemia Group, British Journal of Haematology 92(2) (1996) 370–374.

[22] R. Stasi, M. Brunetti, A. Parma, C. Di Giulio, E. Terzoli, The prognostic value of soluble interleukin-6 receptor in patients with multiple myeloma, Cancer 82(10) (1998) 1860–1866.

[23] J.P. Gaillard, R. Bataille, H. Brailly, C. Zuber, K. Yasukawa, M. Attal, N. Maruo, T. Taga, T. Kishimoto, B. Klein, Increased and highly stable levels of functional soluble interleukin-6 receptor in sera of patients with monoclonal gammopathy, European Journal of Immunology 23(4) (1993) 820–824.

[24] I. Nicoletti, G. Migliorati, M.C. Pagliacci, F. Grignani, C. Riccardi, A rapid and simple method for measuring thymocyte apoptosis by propidium iodide staining and flow cytometry, Journal of Immunological Methods 139(2) (1991) 271–279.

[25] J.W. Oh, M. Revel, J. Chebath, A soluble interleukin 6 receptor isolated from conditioned medium of human breast cancer cells is encoded by a differentially spliced mRNA, Cytokine 8(5) (1996) 401–409.

[26] S. Rose-John, G.H. Waetzig, J. Scheller, J. Grotzinger, D. Seegert, The IL-6/sIL-6R complex as a novel target for therapeutic approaches, Expert Opin Ther Targets 11(5) (2007) 613–624.

[27] J. Wolf, S. Rose-John, C. Garbers, Interleukin-6 and its receptors: a highly regulated and dynamic system, Cytokine 70(1) (2014) 11–20.

[28] M. Fischer, J. Goldschmitt, C. Peschel, J.P. Brakenhoff, K.J. Kallen, A. Wollmer, J. Grotzinger, S. Rose-John, I. A bioactive designer cytokine for human hematopoietic progenitor cell expansion, Nat Biotechnol 15(2) (1997) 142–145.

[29] P. Aigner, V. Just, D. Stoiber, STAT3 isoforms: Alternative fates in cancer?, Cytokine 118 (2019) 27–34.

[30] J. Chen, C. Mao, N. Han, Q. Zhou, C. Feng, X. Sun, Y. Song, Post-translational modifications of Stat3: The state of the art, Cell Signal 135 (2025) 112048.

[31] R. Atreya, J. Mudter, S. Finotto, J. Mullberg, T. Jostock, S. Wirtz, M. Schutz, B. Bartsch, M. Holtmann, C. Becker, D. Strand, J. Czaja, J.F. Schlaak, H.A. Lehr, F. Autschbach, G. Schurmann, N. Nishimoto, K. Yoshizaki, H. Ito, T. Kishimoto, P.R. Galle, S. Rose-John, M.F. Neurath, Blockade of interleukin 6 trans signaling suppresses T-cell resistance against apoptosis in chronic intestinal inflammation: evidence in crohn disease and experimental colitis in vivo, Nat Med 6(5) (2000) 583–588.

[32] T. Jostock, J. Mullberg, S. Ozbek, R. Atreya, G. Blinn, N. Voltz, M. Fischer, M.F. Neurath, S. Rose-John, Soluble gp130 is the natural inhibitor of soluble interleukin-6 receptor transsignaling responses, Eur J Biochem 268(1) (2001) 160–167.

[33] B. Rabe, A. Chalaris, U. May, G.H. Waetzig, D. Seegert, A.S. Williams, S.A. Jones, S. Rose-John, J. Scheller, Transgenic blockade of interleukin 6 transsignaling abrogates inflammation, Blood 111(3) (2008) 1021–1028.

[34] P. Baran, S. Hansen, G.H. Waetzig, M. Akbarzadeh, L. Lamertz, H.J. Huber, M.R. Ahmadian, J.M. Moll, J. Scheller, The balance of interleukin (IL)-6, IL-6.soluble IL-6 receptor (sIL-6R), and IL-6.sIL-6R.sgp130 complexes allows simultaneous classic and trans-signaling, J Biol Chem 293(18) (2018) 6762–6775.

[35] J. Kamińska, M.M. Kowalska, K.J. Nowak, M. Rolewska, J. Dwilewicz-Trojaczek, K. Terlecki, A. Pękala, J. Woźniak, H. Makuch-Łasica, J. Nowak, Serum sIL-6R levels as prognostic factor in multiple myeloma, Acta Haematologica Polonica 46(3) (2015) 203–208.

[36] C.A. Kyriakou, M.G. Alexandrakis, E. Kyriakou, A. Perakis, T.V. Kourelis, M. Chronaki, A.K. Alegakis, T. Kalmantis, D.A. Mavroudis, Serum interleukin-6 and interleukin-6 receptor levels in patients with multiple myeloma, Haematologia 28(2) (1997) 71–79.

[37] W. Thabard, S. Barillé, M. Collette, J.L. Harousseau, M.J. Rapp, R. Bataille, Myeloma cells release soluble interleukin-6Ralpha in relation to disease progression by two distinct mechanisms: alternative splicing and proteolytic cleavage, Clinical Cancer Research 5(9) (1999) 2693–2697.

[38] B. Dankbar, T. Padró, R. Leo, B. Feldmann, M. Kropff, R.M. Mesters, H. Serve, W.E. Berdel, J. Kienast, Vascular endothelial growth factor and interleukin-6 in paracrine tumor-stromal cell interactions in multiple myeloma, Blood 95(8) (2000) 2630–2636.

[39] M.G. Alexandrakis, F.H. Passam, A. Sfiridaki, E. Kandidaki, P. Roussou, D.S. Kyriakou, Elevated serum concentration of hepatocyte growth factor in patients with multiple myeloma: correlation with markers of disease activity, American Journal of Hematology 72(4) (2003) 229–233.

[40] C.E. Hack, E.R. De Groot, R.J. Felt-Bersma, J.H. Nuijens, R.J. Strack Van Schijndel, A.J. Eerenberg-Belmer, L.G. Thijs, L.A. Aarden, Increased plasma levels of interleukin-6 in sepsis, Blood 74(5) (1989) 1704–1710.

[41] T. Hirano, T. Matsuda, M. Turner, N. Miyasaka, G. Buchan, B. Tang, K. Sato, M. Shimizu, R. Maini, M. Feldmann, et al., Excessive production of interleukin 6/B cell stimulatory factor-2 in rheumatoid arthritis, Eur J Immunol 18(11) (1988) 1797–1801.

[42] A. Mohr, T. Chu, C.T. Clarkson, G.N. Brooke, V.B. Teif, R.M. Zwacka, Fas-threshold signalling in MSCs promotes pancreatic cancer progression and metastasis, Cancer Lett 519 (2021) 63–77.

[43] T. Tanaka, M. Narazaki, T. Kishimoto, IL-6 in inflammation, immunity, and disease, Cold Spring Harb Perspect Biol 6(10) (2014) a016295.

[44] A. Waage, P. Brandtzaeg, A. Halstensen, P. Kierulf, T. Espevik, The complex pattern of cytokines in serum from patients with meningococcal septic shock. Association between interleukin 6, interleukin 1, and fatal outcome, J Exp Med 169(1) (1989) 333–338.

[45] D. Chauhan, P. Pandey, A. Ogata, G. Teoh, S. Treon, M. Urashima, S. Kharbanda, K.C. Anderson, Dexamethasone induces apoptosis of multiple myeloma cells in a JNK/SAP kinase independent mechanism, Oncogene 15(7) (1997) 837–843.

[46] W.C. Cheung, B. Van Ness, The bone marrow stromal microenvironment influences myeloma therapeutic response in vitro, Leukemia 15(2) (2001) 264–271.

[47] C. Garbers, S. Heink, T. Korn, S. Rose-John, Interleukin-6: designing specific therapeutics for a complex cytokine, Nature Reviews Drug Discovery 17(6) (2018) 395–412.

[48] D.E. Johnson, R.A. O'Keefe, J.R. Grandis, Targeting the IL-6/JAK/STAT3 signalling axis in cancer, Nature Reviews Clinical Oncology 15(4) (2018) 234–248.

[49] R.Z. Orlowski, L. Gercheva, C. Williams, H. Sutherland, T. Robak, T. Masszi, V. Goranova-Marinova, M.A. Dimopoulos, J.D. Cavenagh, I. Špička, R. Ofori-Asenso, M.-J. Yerna, D. Bhatt, J. Vermeulen, H. van de Velde, M. Ziyad, A phase 2, randomized, double-blind, placebo-controlled study of siltuximab (anti-IL-6 mAb) and bortezomib versus bortezomib alone in patients with relapsed or refractory multiple myeloma, American Journal of Hematology 90(1) (2015) 42–49.

[50] P.M. Voorhees, R.F. Manges, P. Sonneveld, S. Jagannath, G. Somlo, A. Krishnan, S. Lentzsch, R.C. Frank, S. Zweegman, P.W. Wijermans, R.Z. Orlowski, B. Kranenburg, B. Hall, T. Casneuf, X. Qin, H. van de Velde, H. Xie, S.K. Thomas, A phase 2 multicentre study of siltuximab, an anti-interleukin-6 monoclonal antibody, in patients with relapsed or refractory multiple myeloma, Br J Haematol 161(3) (2013) 357–366.

Figure 1

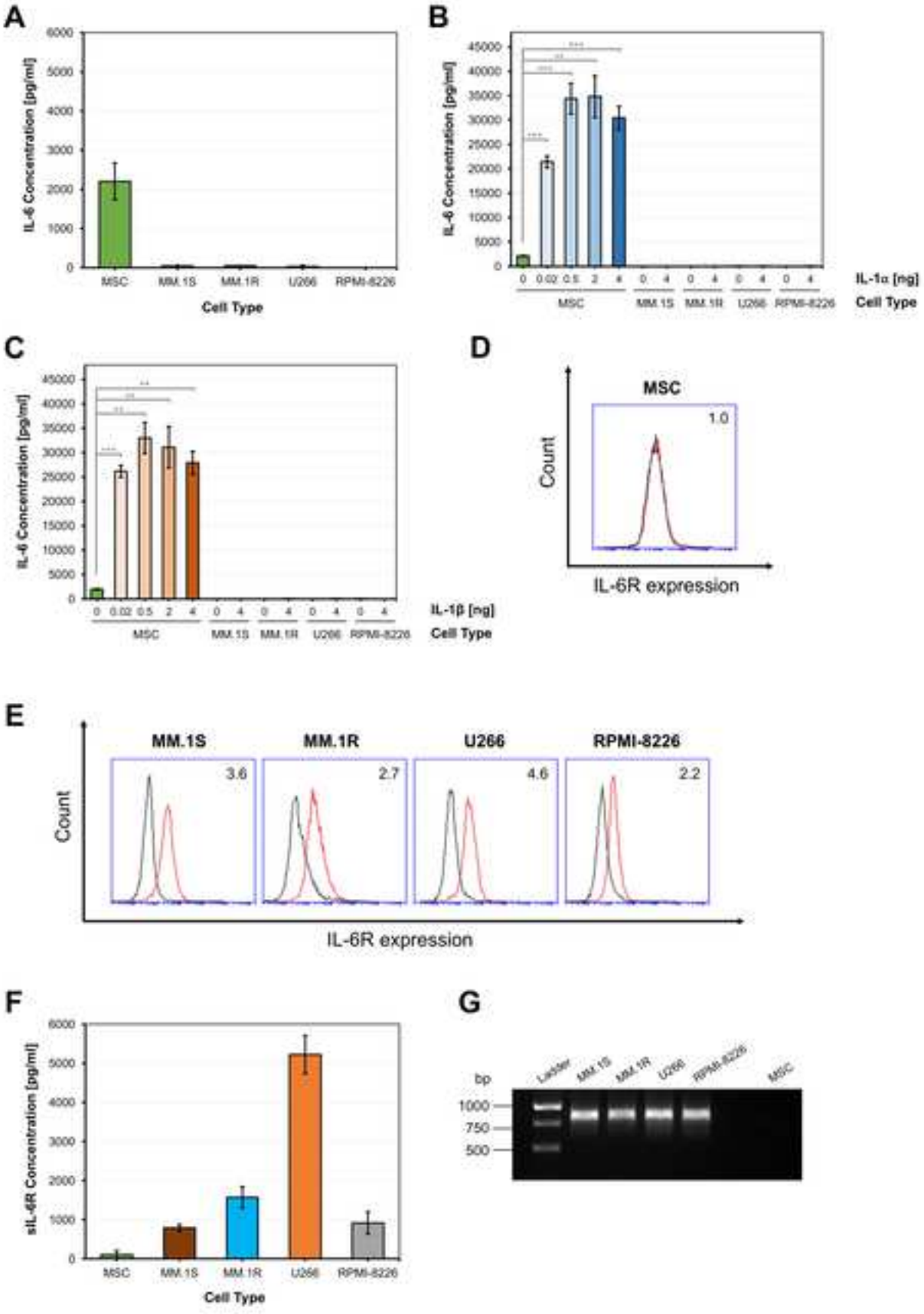
A
IL-6 Concentration [pg/ml]
MSC
MM.1S
MM.1R
U266
RPMI-8226
Cell Type
B
IL-6 Concentration [pg/ml]
IL-1α [ng]
Cell Type
C
IL-6 Concentration [pg/ml]
IL-1β [ng]
Cell Type
D
MSC
1.0
Count
IL-6R expression
E
MM.1S
MM.1R
U266
RPMI-8226
3.6
2.7
4.6
2.2
Count
IL-6R expression
F
sIL-6R Concentration [pg/ml]
Cell Type
G
bp
Ladder
1000
750
500

Figure 2

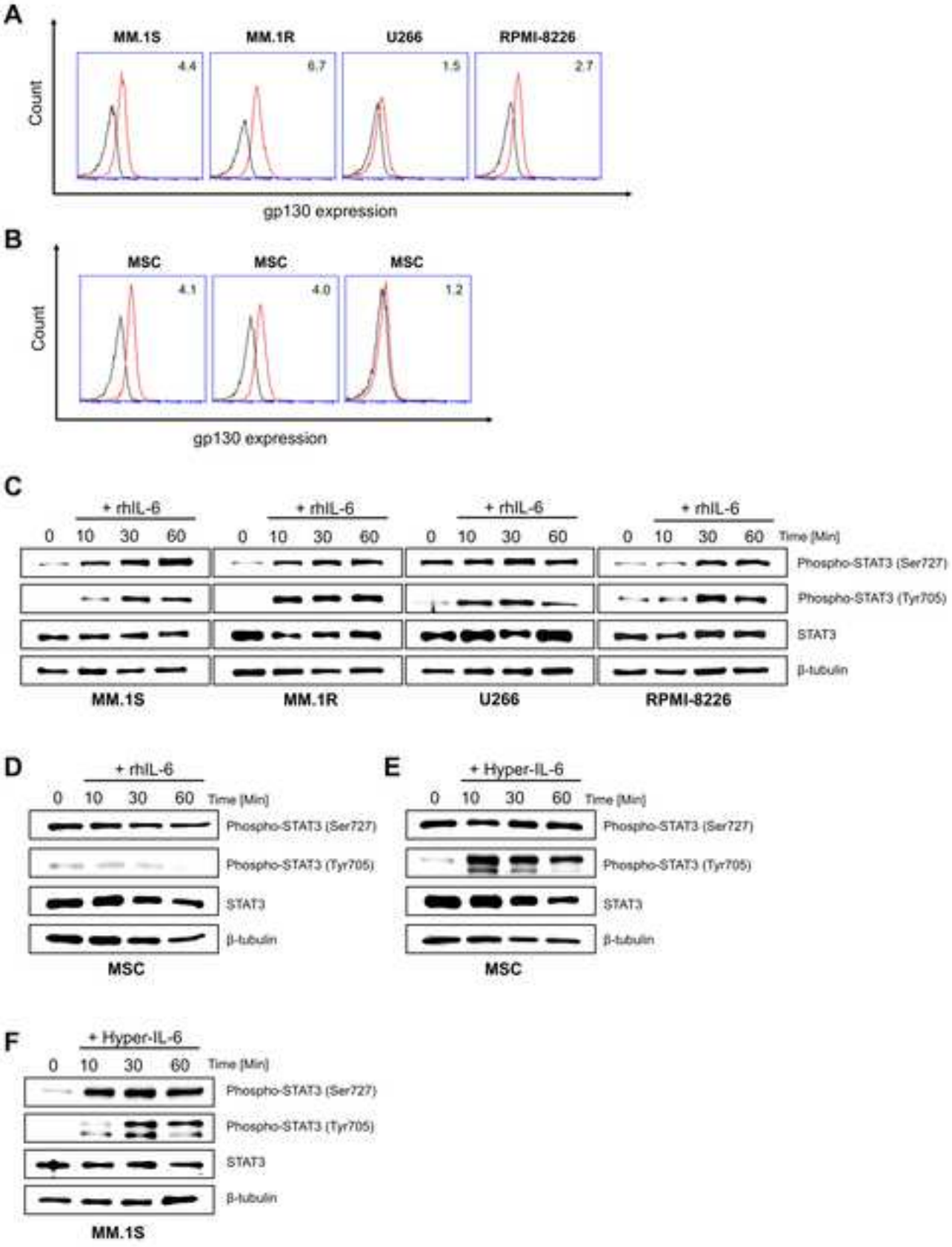
A
MM.1S
MM.1R
U266
RPMI-8226
4.4
6.7
1.5
2.7
Count
gp130 expression
B
MSC
MSC
MSC
4.1
4.0
1.2
Count
gp130 expression
C
+ rhIL-6
0 10 30 60
Time [Min]
Phospho-STAT3 (Ser727)
Phospho-STAT3 (Tyr705)
STAT3
β-tubulin
MM.1S
MM.1R
U266
RPMI-8226
D
+ rhIL-6
0 10 30 60
Time [Min]
Phospho-STAT3 (Ser727)
Phospho-STAT3 (Tyr705)
STAT3
β-tubulin
MSC
E
+ Hyper-IL-6
0 10 30 60
Time [Min]
Phospho-STAT3 (Ser727)
Phospho-STAT3 (Tyr705)
STAT3
β-tubulin
MSC
F
+ Hyper-IL-6
0 10 30 60
Time [Min]
Phospho-STAT3 (Ser727)
Phospho-STAT3 (Tyr705)
STAT3
β-tubulin
MM.1S

Figure 3

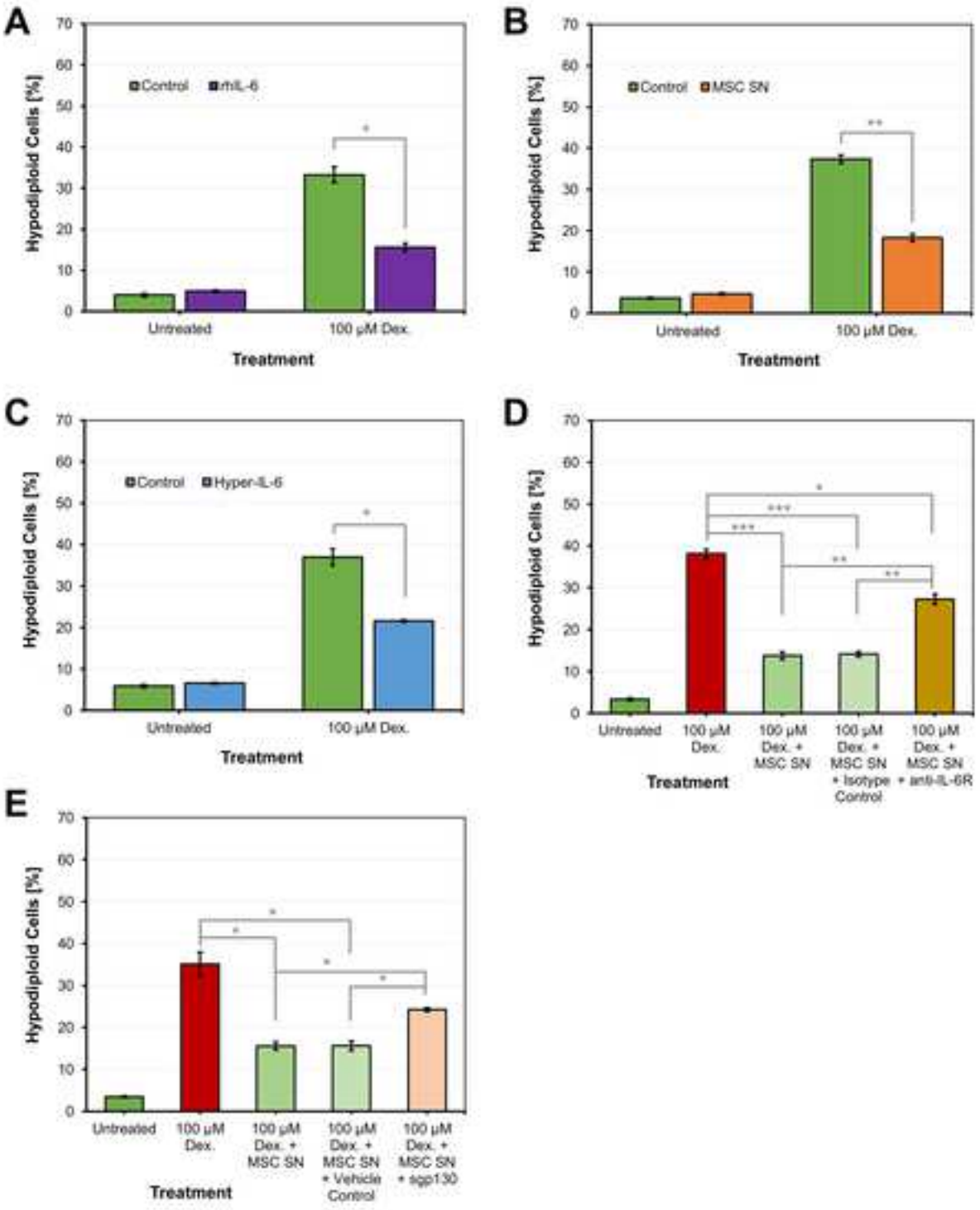
A
Hypodiploid Cells [%]
Control
rhIL-6
Untreated
100 µM Dex.
Treatment
B
Hypodiploid Cells [%]
Control
MSC SN
Untreated
100 µM Dex.
Treatment
C
Hypodiploid Cells [%]
Control
Hyper-IL-6
Untreated
100 µM Dex.
Treatment
D
Hypodiploid Cells [%]
Untreated
100 µM Dex.
100 µM Dex. + MSC SN
100 µM Dex. + MSC SN + Isotype Control
100 µM Dex. + MSC SN + anti-IL-6R
Treatment
E
Hypodiploid Cells [%]
Untreated
100 µM Dex.
100 µM Dex. + MSC SN
100 µM Dex. + MSC SN + Vehicle Control
100 µM Dex. + MSC SN + sgp130
Treatment

Figure 4

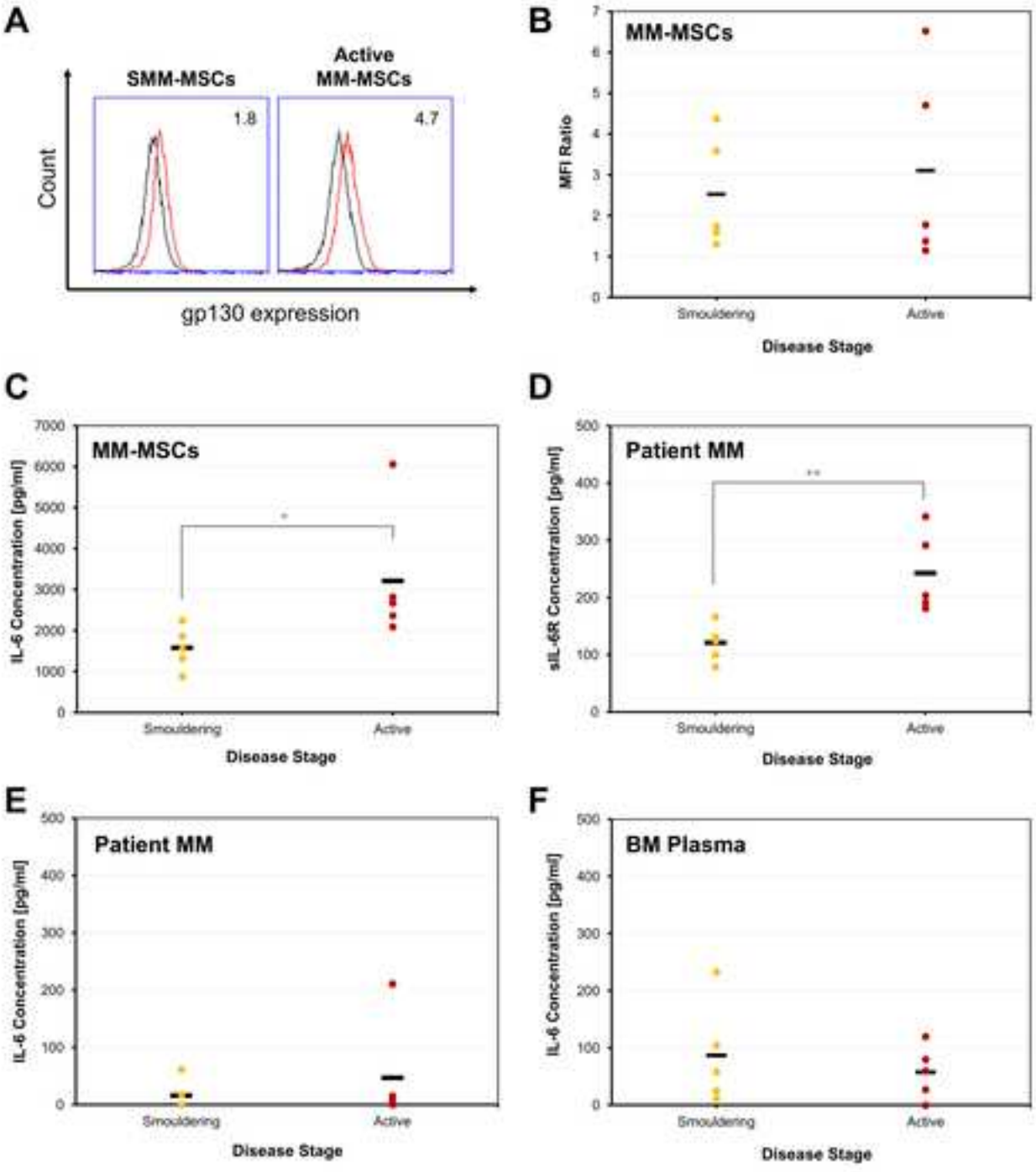
A
SMM-MSCs
Active MM-MSCs
1.8
4.7
Count
gp130 expression
B
MM-MSCs
MFI Ratio
Smouldering
Active
Disease Stage
C
MM-MSCs
IL-6 Concentration [pg/ml]
Smouldering
Active
Disease Stage
D
Patient MM
sIL-6R Concentration [pg/ml]
Smouldering
Active
Disease Stage
E
Patient MM
IL-6 Concentration [pg/ml]
Smouldering
Active
Disease Stage
F
BM Plasma
IL-6 Concentration [pg/ml]
Smouldering
Active
Disease Stage

Figure 5

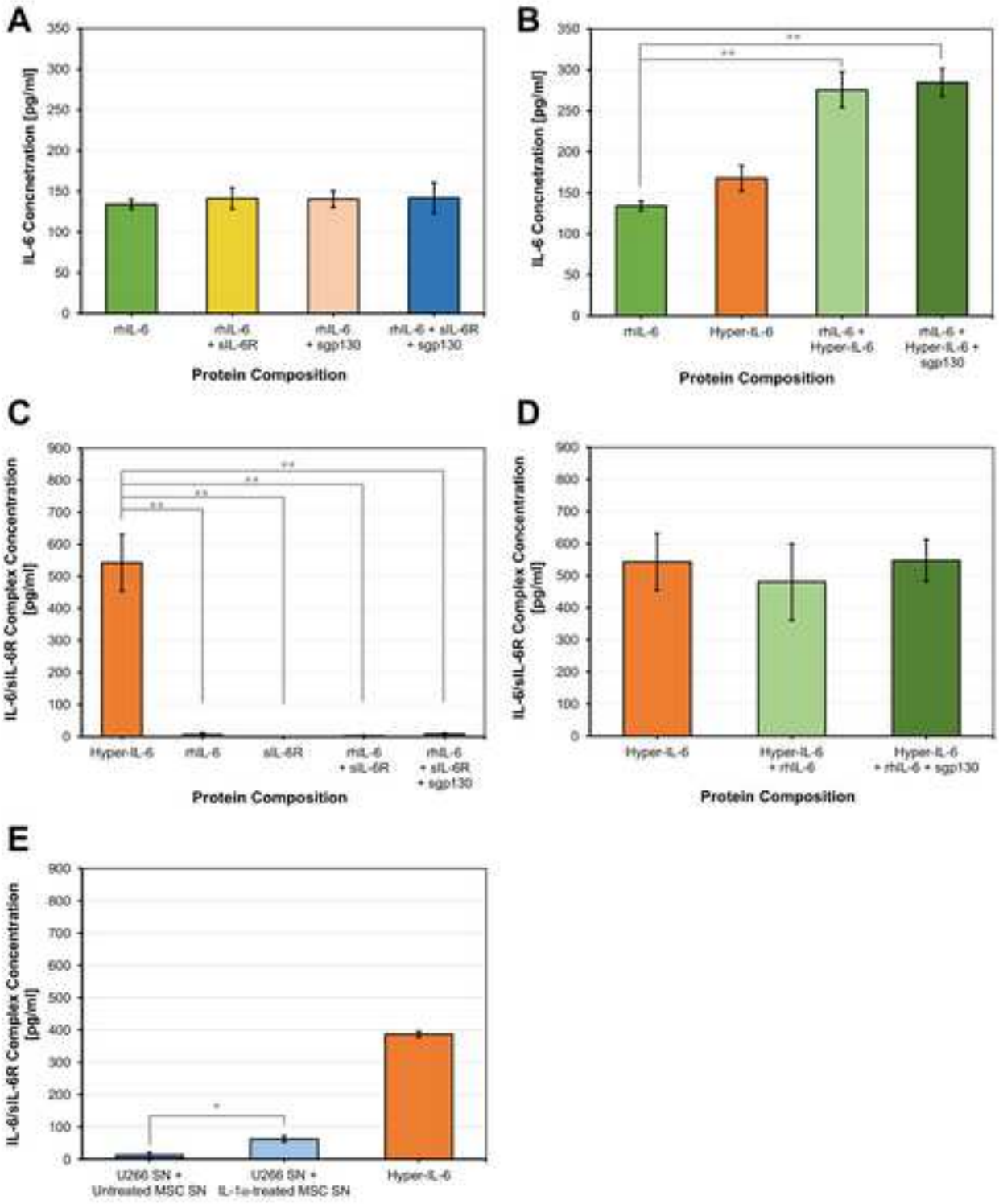
A
IL-6 Concnetration [pg/ml]
rhIL-6
rhIL-6 + sIL-6R
rhIL-6 + sgp130
rhIL-6 + sIL-6R + sgp130
Protein Composition
B
IL-6 Concnetration [pg/ml]
rhIL-6
Hyper-IL-6
rhIL-6 + Hyper-IL-6
rhIL-6 + Hyper-IL-6 + sgp130
Protein Composition
C
IL-6/sIL-6R Complex Concentration [pg/ml]
Hyper-IL-6
rhIL-6
sIL-6R
rhIL-6 + sIL-6R
rhIL-6 + sIL-6R + sgp130
Protein Composition
D
IL-6/sIL-6R Complex Concentration [pg/ml]
Hyper-IL-6
Hyper-IL-6 + rhIL-6
Hyper-IL-6 + rhIL-6 + sgp130
Protein Composition
E
IL-6/sIL-6R Complex Concentration [pg/ml]
U266 SN + Untreated MSC SN
U266 SN + IL-1α-treated MSC SN
Hyper-IL-6